**Carib.J.Sci.Tech**

# Heat and mass transfer in MHD flow of nanofluids through a porous media due to a stretching sheet with viscous dissipation and chemical reaction effects

**Authors & Affiliation:**

**K.Y. Yohannes**

Department of Mathematics, Osmania University,Hyderabad-500 007, Andhra Pradesh, INDIA.

**B. Shankar**

Department of Mathematics, Osmania University,Hyderabad-500 007, Andhra Pradesh, INDIA.


**Correspondence To:**

**K.Y. Yohannes**

**Key Words:**

Magnetohydrodynamic, heat transfer, viscous dissipation, chemical reaction, nanofluid, Soret effect, stretching sheet.

## ABSTRACT

This paper investigates the convective heat and mass transfer in nanofluid flow through a porous media due to a stretching sheet subjected to magnetic field, viscous dissipation, chemical reaction and Soret effects. Two types of nanofluids, namely Cu-water and Ag-water were studied. The governing boundary layer equations are formulated and reduced to a set of ordinary differential equations using similarity transformations and then solved numerically by an explicit finite difference scheme known as the Keller box method. Numerical results were obtained for the skin friction coefficient, Nusselt number, Sherwood number as well as for the velocity, temperature and concentration profiles for selected values of the governing parameters, such as the nanoparticle volume fraction $\phi$, the magnetic parameter M, porous media parameter $K_1$, Eckert number Ec, Soret number Sr, Schmidt number Sc and chemical reaction parameter $\gamma$. Excellent validation of the present numerical results has been achieved with the earlier linearly stretching sheet problems in the literature.

## Introduction

The study of the boundary layer flow of an electrically conducting fluid through a porous media has many applications in manufacturing and natural process which include cooling of electronic devices by fans, cooling of nuclear reactors during emergency shutdown, cooling of an infinite metallic plate in a cooling bath, textile and paper industries, glass-fiber production, manufacture of plastic and rubber sheets, the utilization of geothermal energy, the boundary layer control in the field of aerodynamics, food processing, plasma studies and in the flow of biological fluids.

Magnetohydrodynamics(MHD) is the study of the flow of electrically conducting fluids in a magnetic field. Many experimental and theoretical studies on conventional electrically conducting fluids indicate that magnetic field markedly changes their transport and heat transfer characteristics. The study of magnetohydrodynamics has many important applications, and may be used to deal with problems such as cooling of nuclear reactors by liquid sodium and induction flow meter, which depends on the potential difference in the fluid in the direction perpendicular to the motion and to the magnetic field [1]. Recently, the application of magnetohydrodynamics in the polymer industry and metallurgy has attracted the attention of many researchers. Several researches investigated the MHD flow [2 - 9].

Dissipation is the process of converting mechanical energy of downward-flowing water into thermal and acoustical energy. Viscous dissipation is of interest for many applications: significant temperature rises are observed in polymer processing flows such as injection modeling or extrusion at high rates. Aerodynamic heating in the thin boundary layer around high speed aircraft raises the temperature of the skin. In a completely different application, the dissipation function is used to define the viscousity of dilute suspensions Einstein [10]: Viscous dissipation for a fluid with suspended particles is equated to the viscous dissipation in a pure Newtonian fluid, both being in the same flow (same macroscopic velocity gradient). Vajravelu and Hadjinicolaou [11] analyzed the heat transfer characteristics over a stretching surface with viscous dissipation in the presence of internal heat generation or absorption. The effects viscous dissipation is numerically studied on a boundary layer flow of nanofluids over a moving flat plate is studied by Motsumi and Makinde [12]. Gebhart [13] and Gebhart and Mollendorf [14] studied the effect of viscous dissipation in natural convection processes. They observed that the effect of viscous dissipation is significant in vigorous natural convection and mixed convection processes. They also showed the existence of a similarity solution for the external flow over an infinite vertical surface with an exponential variation of surface temperature. Javed and Sina [15] studied the viscous flow over nonlinearly stretching sheet with effects of viscous dissipation. They found that for large Prandtl numbers, the temperature profile decreases. Habibi et al. [16] studied the mixed convection MHD flow of nanofluid over a non-linear stretching sheet with effects of viscous dissipation and variable magnetic field.

The presence of porous media in a boundary layer flow, can significantly change the flow field and, as a consequence, affect the heat transfer rate at the surface. Porous media are generally modeled using the classical Darcy formulation, which implies that the mean filter velocity is proportional to the summation of the pressure gradient and the gravitational force. The model is empirical and cannot be derived analytically via a momentum on a small element of porous medium. The Darcian model has been widely used non - Newtonian porous media heat transfer flows. For regimes where higher velocities may occur, the Darcy linear model is inadequate and refinements have to be employed. The Darcy Forchheimer (DF) model is probably the most popular modification to Darcian flows utilized in simulating inertial effects. It has been used extensively in chemical engineering analysis and also in materials processing simulations. The flow and heat transfer through a porous media has practical applications especially in geophysical fluid dynamics such as beach sand, wood, sandstone, limestone, the human lung and in small blood vessels [17].

Heat and mass transfer problems with a chemical reaction have received a considerable amount of attention in recent years. In processes such as drying, evaporation, energy transfer in a cooling tower and the flow in a desert cooler, heat and mass transfer occur simultaneously. Natural convection processes involving the combined mechanisms are also encountered in many natural processes and industrial applications, such as

in the curing of plastics, the cleaning and chemical processing of materials and the manufacture of pulp and insulated cables. Chamka [18] studied the MHD flow over a uniformly stretched vertical permeable surface subject to a chemical reaction. Afifi [19] analyzed the MHD free convective flow and mass transfer over a stretching sheet with a homogeneous chemical reaction of order n (where n was taken to be 0, 1, 2 or 3). The influence of a chemical reaction on heat and mass transfer due to natural convection from vertical surfaces in porous media subject to Soret and Dufour effects was studied by Postelnicu [20]. He showed that the thickness of the concentration boundary layer decreases as the Lewis number increases, a phenomenon also evident when a chemical reaction is absent. Kandasamy and Palanimani [21] carried out an analysis of the effects of chemical reactions on heat and mass transfer on a magnetohydrodynamic boundary layer flow over a wedge with ohmic heating and viscous dissipation in a porous medium.

Fluid heating and cooling are important in many industries such as power, manufacturing, transportation, and electronics. Effective cooling techniques are greatly needed for cooling any sort of high-energy device. Common heat transfer fluids such as water, ethylene glycol, and engine oil have limited/poor heat transfer capabilities due to their low heat transfer properties. In contrast, metals have thermal conductivities up to three times higher than these fluids, so it is natural that it would be desired to combine the two substances to produce a heat transfer medium that behaves like a fluid, but has the thermal conductivity of a metal. A lot of experimental and theoretical researches has been made to improve the thermal conductivity of these fluids. In 1993, during an investigation of new coolants and cooling technologies at Argonne national laboratory in U.S, Choi invented a new type of fluid called Nanofluid [22]. Nanofluids are fluids that contain small volumetric quantities of nanometer-sized particles, called nanoparticles. These fluids are engineered colloidal suspensions of nanoparticles in a base fluid [23]. The nanoparticles used in nanofluids are typically made of metals, oxides, carbides, or carbon nanotubes. Common base fluids include water, ethylene glycol and oil. Nanofluids commonly contain up to a 5% volume fraction of nanoparticles to see effective heat transfer enhancements. Nanofluids are studied because of their heat transfer properties:
they enhance the thermal conductivity and convective properties over the properties of the base fluid. Moreover, the presence of the nanoparticles enhance the electrical conductivity property of the nanofluids, hence are more susceptible to the influence of magnetic field than the conventional base fluids. Typical thermal conductivity enhancements are in the range of 15-40% over the base fluid and heat transfer coefficient enhancements have been found up to 40% [24]. Thermophysical properties of nanofluids such as thermal conductivity, diffusivity and viscosity have been studied by, among others, Kang et al. [25], Velagapudi et al. [26] and Rudyak et al. [27].

After the pioneer investigation of Choi, thriving experimental and theoretical researches were undertaken to discover and understand the mechanisms of heat transfer in nanofluids. The knowledge of the physical mechanisms of heat transfer in nanofluids is of vital importance as it will enable the exploitation of their full heat transfer potential. Masuda et al. [28] observed the characteristic feature of nanofluid is thermal conductivity enhancement. This observation suggests the possibility of using nanofluids in advanced nuclear systems [29]. A comprehensive survey of convective transport in nanofluids was made by Buongiorno [30], who says that a satisfactory explanation for the abnormal increase of the thermal conductivity and viscosity is yet to be found. He focused on further heat transfer enhancement observed in convective situations. Khan and Pop [31] presented a similarity solution for the free convection boundary layer flow past a horizontal flat plate embedded in a porous medium filled with a nanofluid. Makinde and Aziz [32] studied MHD mixed convection from a vertical plate embedded in a porous medium with a convective boundary condition.

Majority of the above studies are restricted to boundary layer flow and heat transfer in Newtonian fluids. However, due to the increasing importance of nanofluids, in recent years a great attention has been given to the study of convective transport of nanofluids. In addition to this the flow of nanofluids through a porous media with effects of chemical reaction and viscous dissipation has been given less attention. Therefore, the aim of the present paper is to study the magnetohydrodynamic flow and heat transfer of nanofluids through a porous Media due to a stretching sheet with viscous dissipation and chemical reaction effects. The

combined effect of all the above mentioned parameters has not been reported so far in the literature, which makes the present paper unique.

The governing highly nonlinear partial differential equation of momentum, energy and concentration fields has been simplified by using a suitable similarity transformations and then solved numerically with the help of a powerful, easy to use method called the Keller box method. This method has already been successfully applied to several non linear problems corresponding to a parabolic partial differential equations. As discussed in [33] the exact discrete calculus associated with the Keller-Box Scheme is shown to be fundamentally different from all other mimic numerical methods. The box-scheme of Keller [33], is basically a mixed finite volume method, which consists in taking the average of a conservation law and of the associated constitutive law at the level of the same mesh cell.

The paper is organized as follows: the mathematical formulation of the problem is presented in section 2. Section 3 outlines the numerical procedure whilst results and discussions are presented in section 4. Section 5 concludes the paper.

### Nomenclature

$B_0$ Magnetic induction
C  Nanoparticle concentration
$C_w$ Nanoparticle concentration at the stretching surface
$C_\infty$ Nanoparticle concentration far away from the sheet
$C_f$ Skin-friction coefficient
$c_p$ Specific heat capacity at constant pressure
D  Species diffusivity
$D_1$ The coefficient contribution mass flux through temperature gradient
Ec Eckert number
f  Dimensionless velocity
g  Dimensionless temperature
h  Dimensionless nanoparticle concentration
$k_f$ Thermal conductivity of the base fluid
$k_s$ Thermal conductivity of the nanoperticle
$k_{nf}$ Thermal conductivity of the nanofluid
$K_0$ Chemical reaction parameter
$K_1$ Scaled chemical reaction parameter
$\ell$ Characteristic length
M  Magnetic parameter
$Nu_x$ Nusselt number
Pr  Prandtl number
$Re_x$ Local Reynolds number
$S_x$ Sherwood number
Sc  Schmidt number
Sr  Soret number
T  Fluid temperature
$T_w$ Temperature at the surface
$T_\infty$ Temperature of the fluid far away from the stretching surface

u;v    Velocity components along x-and y-axes, respectively
$u_w$    Velocity of the wall along the x - axes
x;y    Cartesian coordinates measured along stretching surface

**Greek symbols**

$\alpha_{nf}$    Thermal diffusivity of the nanofluid.
$\beta$    Thermal expansion coefficient
$\eta$    Dimensionless similarity variable.
$\gamma$    Scaled chemical reaction parameter.
$\mu_f$    Dynamic viscosity of the base fluid.
$\mu_{nf}$    Dynamic viscosity of the nanofluid fluid.
$\nu_f$    Kinematic viscosity of the base fluid.
$\nu_{nf}$    Kinematic viscosity of the nanofluid.
$\rho_f$    Density of the base fluid.
$\rho_s$    Density of the nanoparticle.
$\rho_{nf}$    Density of the nanofluid.
$(\rho c_p)_f$    Heat capacity of the base fluid.
$(\rho c_p)_s$    Heat capacity of the nanoparticle.
$(\rho c_p)_{nf}$ Heat capacity of the nanofluid.
$\sigma$    Electrical conductivity.
$\phi$    Nanoparticle concentration.

**Subscripts**

$\infty$    Condition at the free stream.
w    Condition at the surface.
f    Base fluid.
s    Nanoparticle.
nf    Nanofluid

**Flow Analysis of the Problem**

Consider the two-dimensional steady laminar flow of an incompressible nanofluid over a stretching sheet. If we consider the cartesian coordinate system with the origin fixed in such a way that, the x-axis is taken along the direction of the continuous stretching surface and the y-axis is measured normal to the surface of the sheet. Two equal but opposite forces are applied along the sheet so that the wall is stretched, keeping the position of the origin unaltered. The fluid is electrically conducting under the influence of an applied magnetic field $B_0(x)$ normal to the stretching surface. Since the magnetic Reynolds number is very small for most fluid used in industrial applications it is assumed that the induced magnetic field is negligible in comparison to the applied magnetic field. The fluid is a water based nanofluid containing two different types of nanoparticles; copper and silver nanoparticles. It is assumed that the base fluid and the nanoparticles are in thermal equilibrium and no slip occurs between them. The thermophysical properties of the nanofluid are given in Table 1 (see Oztop and Abu-Nada [34]). With the above assumptions, the boundary layer equations governing the nanofluid flow, the heat and the concentration fields can be written in dimensional form as [35, 36] If we consider the cartesian coordinate system with the origin fixed in such a way that, the x-axis is taken along the direction of the continuous stretching surface and the y-axis is measured normal to the surface of the sheet. Two equal but opposite forces are applied along the sheet so that the wall is stretched, keeping the position of the origin unaltered. The fluid is electrically conducting under the influence of an applied magnetic field B0(x) normal to the stretching surface. Since the magnetic Reynolds number is very small for most fluid used in industrial applications it is assumed that the induced magnetic field is negligible in comparison to the applied magnetic field. The fluid is a water based nanofluid containing two different types of nanoparticles; copper and silver nanoparticles. It is assumed that the base fluid and the nanoparticles are in thermal equilibrium and no slip occurs between them. The thermophysical properties of the nanofluid are given in Table 1 (see Oztop and Abu-Nada [34]). With the above assumptions, the boundary layer equations governing the nanofluid flow, the heat and the concentration fields can be written in dimensional form as [35, 36]

$$\frac{\partial u}{\partial x} + \frac{\partial v}{\partial y} = 0, \tag{1}$$

$$u\frac{\partial u}{\partial x} + v\frac{\partial u}{\partial y} = \frac{\mu_{nf}}{\rho_{nf}}\frac{\partial^2 u}{\partial y^2} - \frac{\sigma B_0^2(x)}{\rho_{nf}}u - \frac{\mu_{nf}}{\rho_{nf}}\frac{1}{K}u, \tag{2}$$

$$u\frac{\partial T}{\partial x} + v\frac{\partial T}{\partial y} = \alpha_{nf}\frac{\partial^2 T}{\partial y^2} + \frac{\mu_{nf}}{(\rho c_p)_{nf}}\left(\frac{\partial u}{\partial y}\right)^2, \tag{3}$$

$$u\frac{\partial C}{\partial x} + v\frac{\partial C}{\partial y} = D\frac{\partial^2 C}{\partial y^2} + D_1\frac{\partial^2 T}{\partial y^2} - K_0(C_w - C_\infty), \tag{4}$$

Where u and v are the velocity components in the x and y directions respectively, T is the temperature, C is the concentration of the nanofluid , $C_\infty$ is the concentration of the nanofluid far from the sheet $B_0$ is the uniform magnetic field strength, $\sigma$ is the electrical conductivity, $c_p$ is the specific heat at constant pressure,  D is the species diffusivity, $D_1$ is the coefficient that signifies the contribution to mass flux through temperature gradient, K is the permeability of the porous medium, $K_0$ is a chemical reaction parameter; and $\mu_{nf}, \rho_{nf}, \alpha_{nf}$, and $(\rho c_p)_{nf}$ are the dynamic viscosity , density, thermal diffusivity , and heat capacitance of the nanofluid, respectively, which are given as [36, 37]

$$\nu_f = \frac{\mu_f}{\rho_f}, \rho_{nf} = (1 - \phi)\rho_f + \phi\rho_s, \alpha_{nf} = \frac{k_{nf}}{(\rho c_p)_{nf}}, \mu_{nf} = \frac{\mu_f}{(1-\phi)^{2.5}},$$

$$(\rho c_p)_{nf} = (1 - \phi)(\rho c_p)_f + \phi(\rho c_p)_s, \frac{k_{nf}}{k_f} = \frac{(k_s + 2k_f - 2\phi(k_f - k_s))}{(k_s + 2k_f + \phi(k_f - k_s))} \tag{5}$$

In which $\nu_f, \mu_f, \rho_f$, and $k_f$ are the kinematic viscosity, dynamic viscosity, density, ad thermal conductivityof the base fluid respectively; $\rho_s, k_s, (\rho c_p)_s$ are the density, thermal conductivity and heat capacitance of the nanoparticle respectively; $\phi$ is the solid volume fraction of nanoparticles.

The associated boundary conditions to the flow problem can be written as

$$u = u_w = bx, v = 0, T = T_w = T_\infty + A\left(\frac{x}{\ell}\right)^2, C = C_w = C_\infty + B\left(\frac{x}{\ell}\right)^2 \text{ at } y = 0,$$

$$u \to 0, \ T \to T_\infty, \ C \to C_\infty \text{ as } y \to \infty. \tag{6}$$

In which A, B and b are constants, $\ell$ is the characteristic length $T_w$ and $C_w$ are the temperatures and concentration of the sheet, respectively $T_\infty$ and $C_\infty$ are the temperature and concentration of the nanofluid far away from the sheet, respectively.

The continuity equation is satisfied by introducing a stream function $\psi(x, y)$ such that

$$u = \frac{\partial \psi}{\partial y}, \; v = -\frac{\partial \psi}{\partial x} \tag{7}$$

Introducing the following similarity transformations

$$\eta = y \sqrt{\frac{b}{v_f}}, \; u = bxf'(\eta), \; v = -\sqrt{bv_f}\, f(\eta),$$

$$g(\eta) = \frac{T - T_\infty}{T_w - T_\infty}, \; h(\eta) = \frac{C - C_\infty}{C_w - C_\infty} \tag{8}$$

Making use of Eq. (8), the continuity equation (1) is automatically satisfied and equations 2), (3), (4) and (6) reduce to

$$f''' + \phi_1 \left( f f'' - (f')^2 - \frac{M}{\phi_2} f' \right) - K_1 f' = 0, \tag{9}$$

$$g'' + \phi_3 \frac{k_f}{k_{nf}} Pr \left[ fg' - 2f'g + \frac{Ec}{\phi_4} (f')^2 \right] = 0, \tag{10}$$

$$'' - Sc \left[ 2f' \quad - f \quad ' + \gamma \quad \right] + Srg'' = 0 \tag{11}$$

With boundary condition

$$f(0) = 0, \; f'(0) = 1, \; g(0) = 1, \; h(0) = 1,$$
$$f(\eta) \to 0, \; g(\eta) \to 0, \; h(\eta) \to 0, \text{ as } \eta \to \infty \tag{12}$$

Where $f(\eta)$, $g(\eta)$, and $h(\eta)$ are the dimensionless velocity, temperature and nanoparticle concentration, respectively, primes denote differentiation with respect to the similarity variable $\eta$, and

$M = \frac{\sigma B_0^2}{b \rho_{nf}}$, (Magnetic parameter), $K_1 = \frac{v_f}{bK}$, (Porous medium parameter)

$Pr = \frac{v_f}{\alpha_f}$, (Prandtl number), $Ec = \frac{U_w^2}{(c_p)_f (T_w - T_\infty)}$, (Eckert number), $Sc = \frac{v_f}{D}$, (Schmidt number)

$\gamma = \frac{K_0}{b}$, (Scaled chemical reaction parameter), $Sr = \frac{D_1}{D} \frac{(T_w - T_\infty)}{(C_w - C_\infty)}$, (Soret number)

The physical quantities of interest in this problem are the local skin friction coefficient $C_f$, the Nusselt number $Nu_x$, which represents the rate of heat transfer at the surface of the plate and the local Sherwood number $S_x$, which represents the rate of mass transfer at the surface of the plate, which are defined as

$$C_f = \frac{2\tau_w}{\rho_f u_w^2}, \; Nu_x = \frac{xq_w}{k_f (T_w - T_\infty)}, \; S_x = \frac{xJ_w}{D(C_w - C_\infty)} \tag{13}$$

Where $\tau_w$ is the skin friction, $q_w$ is the heat flux and $J_w$ is the mass flux through the plate, which are given by

$$\tau_w = -\mu_{nf} \left( \frac{\partial u}{\partial y} \right)_{y=0}, \; q_w = -k_{nf} \left( \frac{\partial T}{\partial y} \right)_{y=0}, \; J_w = -D \left( \frac{\partial c}{\partial y} \right)_{y=0} \tag{14}$$

Making use of Eq. (8) and (5) in (13), the dimensionless skin friction coefficient, wall heat and mass transfer rates are obtained as

$$C_f (1 - \phi)^{2.5} \sqrt{Re_x} = -2f''(0), \; \frac{Nu_x}{\sqrt{Re_x}} \frac{k_f}{k_{nf}} = -g'(0), \; \frac{S_x}{\sqrt{Re_x}} = - \; '(0) \tag{15}$$

Where $Re_x = \frac{u_w x}{v_f}$ is the local Rynolds number.

**Numerical Solution**

The non linear boundary value problem represented by equations (9) - (11) and (12) are solved numerically using the Keller box method. In solving the system of non linear ordinary differential equations (9) - (11)

together with the boundary condition (12) using the Keller box method the choice of an initial guess is very important. The success of the scheme depends greatly on how much good this guess is to give the most accurate solution. Thus, we made an initial guess of

$$f_0(\eta) = 1 - e^{-\eta}, \; g_0(\eta) = e^{-\eta}, \; h_0(\eta) = e^{-\eta} \qquad (16)$$

These choices have been made based on the convergence criteria together with the boundary conditions in consideration. As in Cebeci and Pradshaw [38], the values of the wall shear stress, in our case $f''(0)$ is commonly used as a convergence criteria. This is because in the boundary layer flow calculations the greatest error appears in the wall shear stress parameter. In the present study this convergence criteria is used. In this study a uniform grid of size $\Delta\eta = 0.01$ is chosen to satisfy the convergence criteria of $10^{-4}$, which gives about a four decimal places accuracy for most of the prescribed quantities.

**Results and Discussion**

We have studied heat and mass transfer in nanofluids flow due to a stretching sheet in porous medium with magnetic field, viscous dissipation, chemical reaction and Soret effects. We considered two different types of nanoparticles, namely, copper and silver, with water as the base fluid (i.e. with a constant Prandtl number Pr = 6.2). The transformed non linear equations (9) - (11) subjected to the boundary condition (12) was solved numerically using Keller box method, which is described in Cebeci and Bradshaw [38]. The velocity, temperature, and concentration profiles were obtained and utilized to compute the skin-friction coefficient, the local Nusselt number, and local Sherwood number in equation (17). The numerical results for different values of the governing parameters viz., nanoparticle concentration $\phi$, magnetic parameter M, porous medium parameter $K_1$, viscous dissipation parameter (Eckert number) Ec, Schmidt number Sc, Soret number Sr, and scaled chemical reaction parameter $\gamma$ are presented in graphs. In the absence of magnetic field, porous media, and chemical reacts effects, to validate the accuracy of our results a comparison has been made with previously reported work by Hamad [39] and Grubka and Bobba [40]. The comparisons are found to be in an excellent agreement (see Tables 2 and 3).

The skin friction coefficients for different values of the magnetic parameter M and nanoparticle volume fraction $\phi$ are given in Table 2. Increasing values of M results in a considerable opposition to the flow due to a Lorenz drag force which increases the values of the skin friction coefficient. The results show a good agreement with Hamad [39].

The heat transfer coefficients are shown in Table 3 for different Prandtl number Pr. It is clear that the heat transfer coefficient increases with Prandtl numbers. The present results are in good agreement with the earlier findings by Grubka and Bobba [40].

**Table 1: Theromphysical physical properties of water, Copper and Silver [34].**

| Physical Properties | Fluid Phase (water) | Cu | Ag |
|---|---|---|---|
| $\rho$ (kg/$m^3$) | 997.1 | 8933 | 10500 |
| $c_p$ (J/kgK) | 4179 | 385 | 235 |
| $k$ (W/mK) | 0.613 | 401 | 429 |

**Table 2: Comparison of the skin friction coefficient $-f''(0)$ for different values of M and $\phi$ when Pr = 6.2 with Hamad [39]**

| M | $\phi$ | Cu-water | | Ag-water | |
|---|---|---|---|---|---|
| | | [39] | Present | [39] | Present |
| 0 | 0.05 | 1.10892 | 1.1089 | 1.13966 | 1.1397 |
| | 0.1 | 1.17475 | 1.1747 | 1.22507 | 1.2251 |
| | 0.15 | 1.20886 | 1.2089 | 1.27215 | 1.2722 |
| | 0.2 | 1.21804 | 1.2180 | 1.28979 | 1.2898 |
| 0.5 | 0.05 | 1.29210 | 1.2921 | 1.31858 | 1.3186 |
| | 0.1 | 1.32825 | 1.3282 | 1.37296 | 1.3730 |
| | 0.15 | 1.33955 | 1.3396 | 1.39694 | 1.3969 |
| | 0.2 | 1.33036 | 1.3304 | 1.39634 | 1.3963 |
| 1 | 0.05 | 1.45236 | 1.4524 | 1.47597 | 1.4760 |
| | 0.1 | 1.46576 | 1.4658 | 1.50640 | 1.5064 |
| | 0.15 | 1.45858 | 1.4586 | 1.51145 | 1.5115 |
| | 0.2 | 1.43390 | 1.4339 | 1.49532 | 1.4953 |
| 2 | 0.05 | 1.72887 | 1.7289 | 1.74875 | 1.7487 |
| | 0.1 | 1.70789 | 1.7079 | 1.74289 | 1.7429 |
| | 0.15 | 1.67140 | 1.6714 | 1.71773 | 1.7177 |
| | 0.2 | 1.62126 | 1.6213 | 1.67583 | 1.6758 |

**Table 3: Comparison the  wall heat transfer rate $-g'(0)$ for various values of Prandtl number Pr, when $\phi = M = K_1 = Ec = 0$ [40]**

| Pr | 0.72 | 1 | 3 | 10 | 100 |
|---|---|---|---|---|---|
| Grubka and Bobba [40] | 1.0885 | 1.3333 | 2.5097 | 4.7969 | 15.7120 |
| Present study | 1.0886 | 1.3333 | 2.5097 | 4.7970 | 15.7198 |

Figures 1 - 3 show, the effect of nanoparticle volume fraction parameter $\phi$ on the nanofluids velocity, temperature and concentration profiles, respectively, in the case of a Cu-water and an Ag-water nanofluids. It is observed that, as the nanoparticle volume fraction increases, the velocity of the nanofluid decreases while the temperature and concentration increase. It is also observed that, the temperature is higher in Ag-water nanufluid than in Cu-water nanofluid, where as the concentration distribution is higher near the boundary and lesser far away from the boundary in the Cu-water than in Ag-water nanofluid. This is due to the fact that as the nanoparticle volume fraction increases the reaction becomes increasingly confined to a relatively narrow region

far from the wall. In addition to this, when the volume fraction of the nanoparticle increases, the thermal conductivity increases, and the thermal boundary layer increases. The velocity in the case of a Cu-water nanofluid is higher than that of Ag-water nanofluid. Since the thermal conductivity of Ag is more than that of Cu, the temperature distribution in Ag-water nanofluid is higher than that of a Cu-water nanofluid. With increasing nanoparticle volume fraction, the thermal boundary layer thickness increases and the velocity boundary layer thickness decreases for both types of nanofluids.

The effect of the viscous dissipation parameter Ec on the temperature profile in the case of Cu-water nanofluid is shown in Figure 4. It is clear that the temperature distribution increases with an increase in the viscous dissipation parameter Ec.

Fig. 5 shows, the effects porosity parameter $K_{1}$ on the velocity of the Cu-water nanofluid. It is observed that the velocity distribution decreases with increasing the porosity parameter. This is because the presence of a porous medium increases the resistance to the flow causing a decrease in the fluid velocity. One can see from Fig.6 that, $g(\eta)$ decreases with an increase of the chemical reaction parameter $\gamma$ in the case of the Cu-water nanofluid. The influence of Sc on $g(\eta)$ for Cu-water nanofluid is shown in  Fig. 7. It is clear that the concentration decreases with an increase in Schmidt number.

The effects of various parameters on the wall skin friction, heat and mass transfer rates are shown in Figs. 8 - 11. Figure 8 illustrates, the effects of the porosity parameter $K_{1}$ and nanoparticle volume fraction $\phi$ on the wall skin friction. It is observed that the skin friction coefficient increases with increasing in the porosity parameter and nanoparticle volume fraction for both the Cu-water and Ag-water nanofluids.

The wall skin friction is higher in the Ag-water nanofluid compared to the Cu-water nanofluid. Thus, the Ag-water nanofluid gives a higher drag force in opposition to the flow as compared to the Cu-water nanofluid. The effects of the viscous dissipation parameter and nanoparticle volume fraction is shown in Fig. 9. It is clear that, the wall heat transfer rate decreases with increasing the viscous dissipation parameter and nanoparticle volume fraction. In addition to this the rate of heat transfer at the wall is higher in Cu-water nanofluid than in Ag-water nanofluid.  The effect of a magnetic field M and porous media parameter $K_{1}$ on the wall heat transfer rate $-g'(0)$ is shown in Fig. 10 in the case of Cu-water and Ag-water nanofluids. The influence of a magnetic field is to reduce the wall heat transfer rates. The porous media effect reduces the wall heat transfer rate. Moreover, the rate of heat transfer at the wall is less in case of the Ag-water nanofluid compared to the Cu-water nanofluid.

The combined effect of the magnetic field and the viscous dissipation parameter(see Figs. 9 and 10) is to generate more heat in the boundary layer region and hence to reduce the wall heat transfer rate. Fig. 11 depicts that, the wall mass transfer rate increases with increase in the chemical reaction parameter and nanoparticle volume fraction for both the Cu-water and Ag-water nanofluids. It is also observed that the rate of mass transfer is higher in the Ag-water nanofluid than in Cu-water nanofluid . The combined effect of the Soret number and Schmidt number on the wall mass transfer rate is shown in Fig. 12 in case of Cu-water and Ag-water nanofluids. It is observed that, the rate of mass transfer in the wall, $h'(0)$ is  an increasing function of Soret number and Schmidt number.
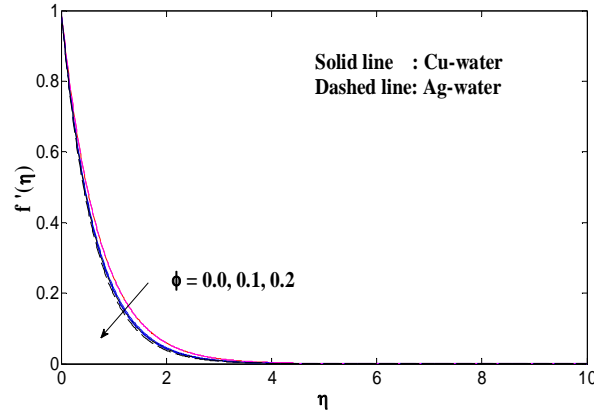
**Figure 1: Effects of $\phi$ on the Velocity profile $f'(\eta)$, when $M = 0$, $K_1 = 1$, $Pr = 6.2$, $Ec = 1$, $Sc = 1$, $\gamma = 0,.08$, $Sr = 0.2$ in case of Cu-water and Ag-water nanofluids.**
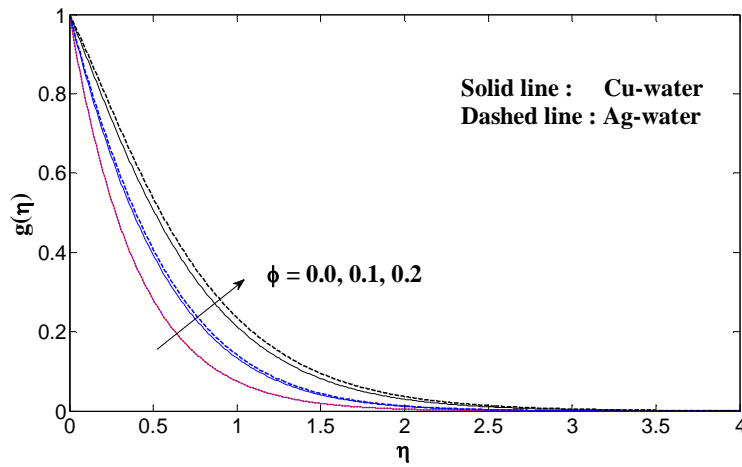


**Figure 2: Effects of $\phi$ on the temperature profile $g(\eta)$, when $M = 0$, $K_1 = 1$, $Pr = 6.2$, $Ec = 1$, Sc= 0, $\gamma = 0,.08$, $Sr = 0.2$ in case of Cu-water and Ag-water nanofluids.**
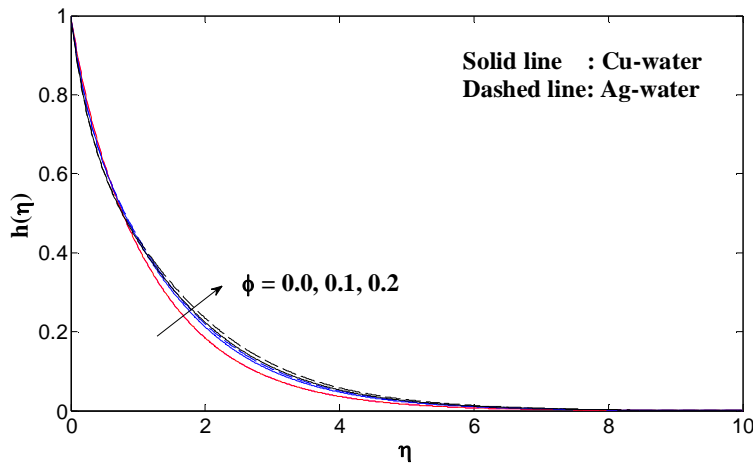


**Figure 3: Effects of $\phi$ on the concentration profile $h(\eta)$, when $M = 0$, $K_1 = 1$, $Pr = 6.2$, $Ec = 1$, $Sc = 0$, $\gamma = 0,.08$, $Sr = 0.2$ in case of Cu-water and Ag-water nanofluids.**
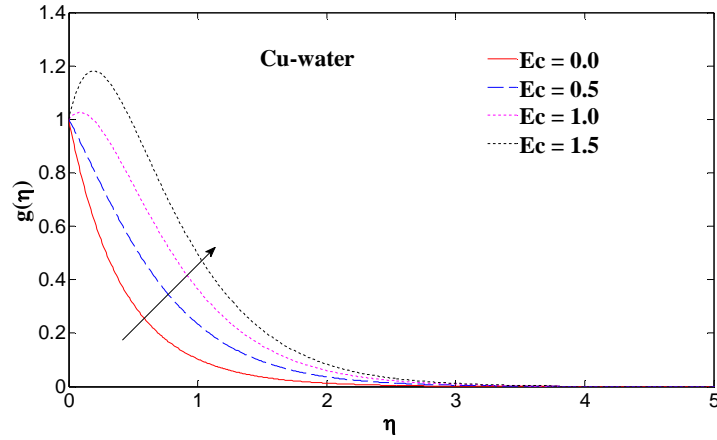
**Figure 4: Effects of $Ec$ on the temperature profile g($\eta$), when $\phi = 0.2$, $M = 0$, $K_1 = 1$, $Pr = 6.2$, $\gamma = 0,.08$, $Sr = 0.2$ in case of Cu-water and Ag-water nanofluids.**
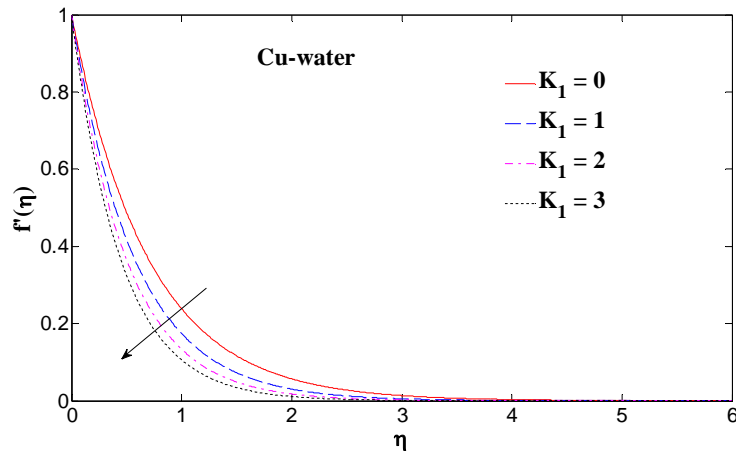


**Figure 5: Effects of $K_1$ on the Velocity profile $f'(\eta)$, when $= 0.2$, $M = 1$, $Pr = 6.2$, $Ec = 1$, $Sc = 1$, $\gamma = 0,.08$, $Sr = 0.2$ in case of Cu-water and Ag-water nanofluids**
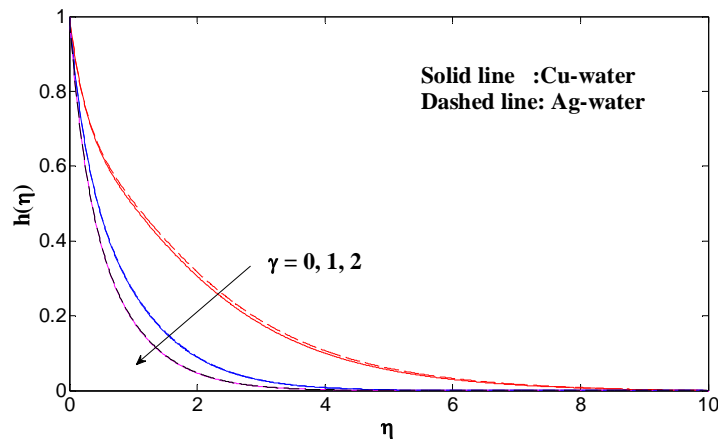


**Figure 6: Effects of $\gamma$ on the concentration profile $h(\eta)$, when $\phi = 0.2$, $M = 1$, $K_1 = 1$, $Pr = 6.2$, $Ec = 1$, $Sc = 1$, $Sr = 0.2$ in case of Cu-water and Ag-water nanofluids.**
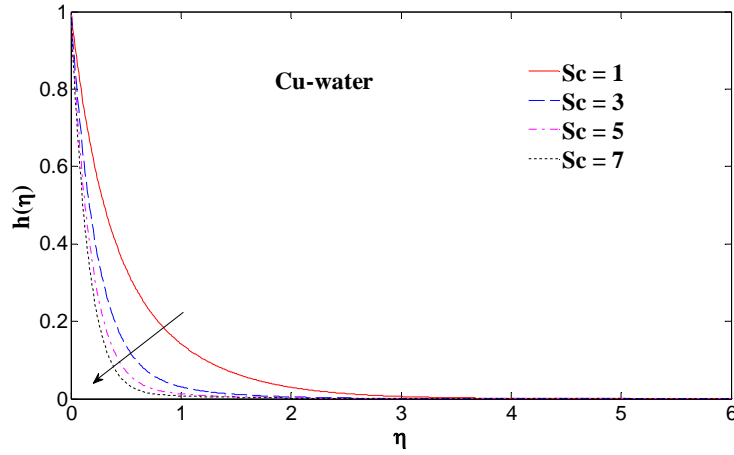
**Figure 7: Effects of $Sc$ on the concentration profile $h(\eta)$, when $\phi = 0.2$, $M = 1$, $K_1 = 1$, $Pr = 6.2$, $Ec = 1$, $\gamma = 0.08$, $Sr = 0.2$ in case of Cu-water nanofluid.**
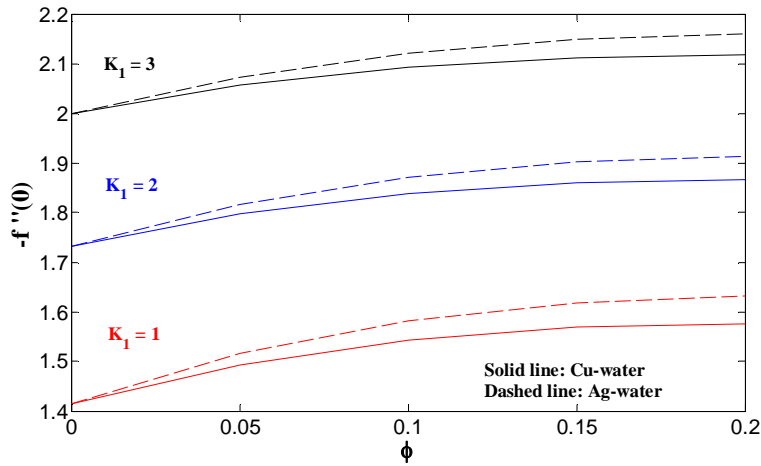


**Figure 8: Effects of $\phi$ on the skin friction coefficient $f''(0)$ for different values of $K_1$, when $M = 0$, $Pr = 6.2$, $Ec = 1$, $Sc = 1$, $\gamma = 0,.08$, $Sr = 0.2$ in case of Cu-water and Ag-water nanofluids.**
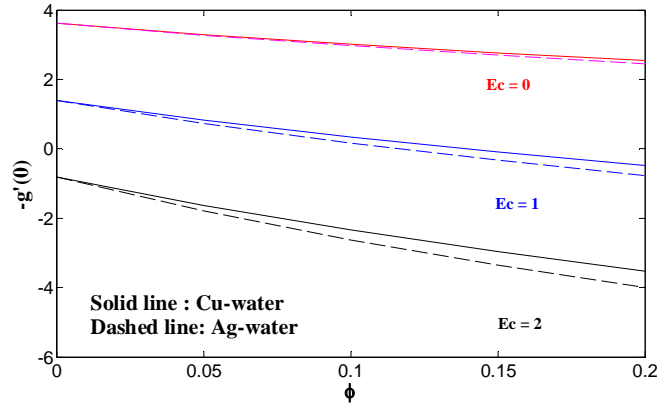
**Figure 9: Effects of $\phi$ on the rate of heat transfer g′(0) for different values of , when $M = 0$, $K_1 = 1$, $Pr = 6.2, Ec = 1, Sc = 1, \gamma = 0,.08, Sr = 0.2$ in case of Cu-water and Ag-water nanofluids**
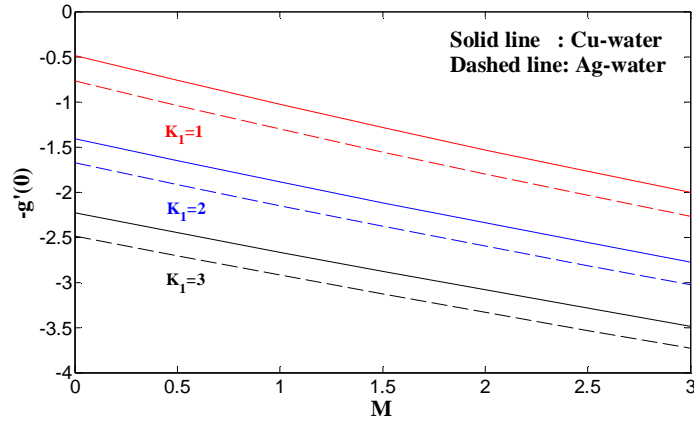


**Figure 10: Effects of $M$ on the rate of heat transfer g′(0) for different values of $K_1$ , when $\phi = 0.2, Pr = 6.2, Ec = 1, Sc = 1, \gamma = 0,.08, Sr = 0.2$ in case of Cu-water and Ag-water nanofluids**
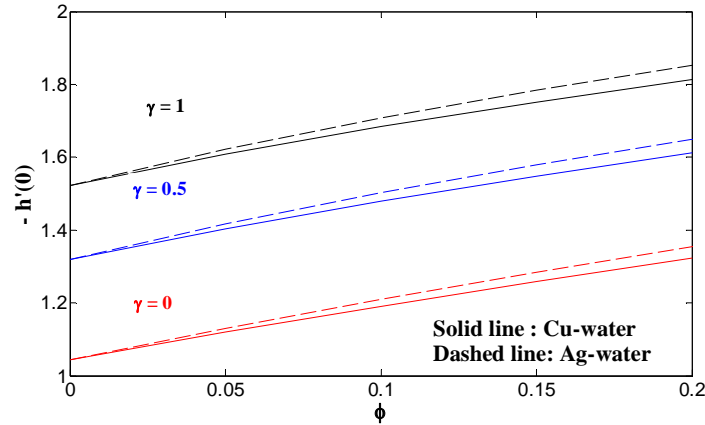
**Figure 11: Effects of $\phi$ on the rate of mass transfer $h'(0)$ for different values of $\gamma$, when $M = 0$, $K_1 = 1$, $Pr = 6.2$, $Ec = 1$, $Sc = 1$, $Sr = 0.2$ in case of Cu-water and Ag-water nanofluids**
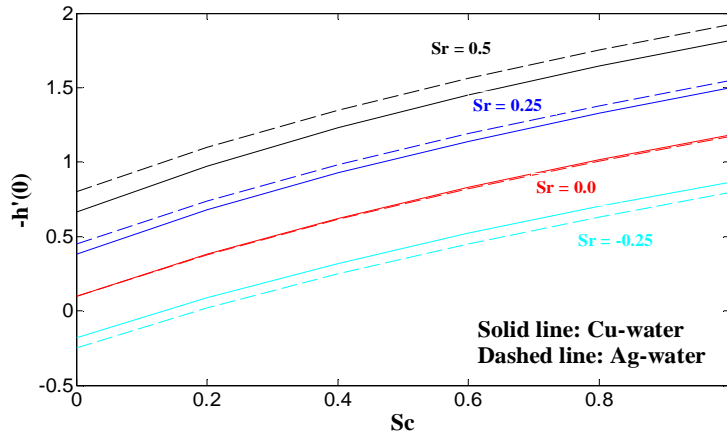


**Figure 12: Effects of $Sc$ on the rate of mass transfer $h'(0)$ for different values of $Sr$, when $\phi = 0.2$, $M = 0$, $K_1 = 1$, $Pr = 6.2$, $Ec = 1$, $\gamma = 0.08$ in case of Cu-water and Ag-water nanofluids**

**Conclusions**

This paper presents the problem MHD flow, heat and mass transfer of nanofluids through a porous medium due a stretching sheet in the presence of viscous dissipation, chemical reaction and soret effects. The governing nonlinear partial differential equations were transformed into ordinary differential equations using the similarity approach and solved numerically using the Keller box method. Two types of nanofluids were considered, Cu-water and Ag-water, and our results revealed, among others, the following.

- The Cu-water nanofluid shows a thicker velocity boundary layer than Ag-water nanofluid. The velocity boundary layer thickness decreases with increasing the nanoparticle volume fraction and porous medium parameter.

- The Ag-water nanofluid shows a thicker thermal boundary layer than Cu-water nanofluid. The thermal boundary layer thickness increases with increasing the values of $\phi$ and Ec.

- The Ag-water nanofluid shows a slightly thicker concentration boundary layer than Cu-water nanofluid. The concentration boundary layer thickness increases with increasing the values of $\phi$ while it decreases with increasing the values of the Sc and $\gamma$.
- The skin friction at the surface increases with increasing the nanoparticle volume fraction and porous medium parameter. The Ag-water nanofluid shows a higher skin friction than Cu-water nanofluid.
- The heat transfer rate at the plate surface decreases with increasing the nanoparticle volume fraction, magnetic field parameter, porous medium parameter and Eckert number. The Cu-water nanofluid has a higher rate of heat transfer than the Ag-water nanofluid.
- The mass transfer rate at the plate surface increases with increasing the nanoparticle volume fraction, Schmidt number, Chemical reaction parameter and Soret number. The Ag-water nanofluid has higher rate of mass transfer than the Cu-water nanofluid.

**References**

1. P. Ganesan and G. Palani, Finite difference analysis of unsteady natural convection MHD flow past an inclined plate with variable surface heat and mass flux, International Journal of Heat and Mass Transfer, 47(19-20)(2004) 4449–4457.
2. K. Jafar, R. Nazar, A. Ishak, and  I. Pop, MHD Flow and Heat Transfer Over stretching/shrinking sheets with external magnetic field, viscous dissipation and Joule Effects, Can. J. Chem. Eng. 9999 (2011) 1–11.
3. M.A.A. Hamada, I. Pop and A.I. Md Ismail, Magnetic field effects on free convection flow of a nanofluid past a vertical semi-infinite flat plate, Nonlinear Anal. Real World Appl. 12 (2011) 1338–1346.
4. H.I. Andersson, An exact solution of the NavierStokes equations for magnetohydrodynamic flow, Acta Mech. 113 (1995) 241–244.
5. K.V. Prasad, D. Pal, V. Umesh and N..S. Prasanna Rao, The effect of variable viscosity on MHD viscoelastic fluid flow and heat transfer over a stretchingsheet, Commun. Nonlinear Sci. Numer. Simul. 15 (2) (2010) 331–334.
6. Beg, A.Y. Bakier and  V.R. Prasad, Numerical study of free convection magnetohydrodynamic heat and mass transfer from a stretching surface to a saturated porous medium with Soret and Dufour effects, Comput. Mater. Sci. 46 (2009) 57–65.
7. T. Fang and J. Zhang, Closed-form exact solutions of MHD viscous flow over a shrinking sheet, Commun. Nonlinear Sci. Numer. Simul. 14 (7) (2009) 2853– 2857.
8. T. Fang, J. Zhang and S. Yao, Slip MHD viscous flow over a stretching sheet – an exact solution, Commun. Nonlinear Sci. Numer. Simul. 14 (11) (2009) 3731– 3737.
9. T. Fang, J. Zhang and S. Yao, Slip magnetohydrodynamic viscous flow over a permeable shrinking sheet, Chin. Phys. Lett. 27 (12) (2010)124702.
10. Einstein,  Ann. phys., 19, 286(1906).
11. K. Vajravelu and A. Hadjinicolaou, Heat transfer in a viscous fluid over a stretching sheet with viscous dissipation and internal heat generation, Int. Comm. in Heat and Mass Transfer, 20(3) (1993) 417–430.
12. T. G. Motsumi and  O. D. Makinde, Effects of thermal radiation and viscous dissipation on boundary layer flow of nanofluids over a permeable moving flat plate, Phys. Scr. 86 (2012) 045003 (8pp).
13. B. Gebhart, Effect of viscous dissipation in natural convection, J. Fluid Mech. 14 (1962) 225–232.
14. B. Gebhart and J. Mollendorf, Viscous dissipation in external natural convection flows, J. Fluid Mech. 38 (1969) 97–107.
15. Javad, and S. Sina, viscous flow over nonlinearly stretching sheet with effects of viscous dissipation, J. Appl. Math. (2012) 1–10. ID 587834.

16. M. Habibi Matin, M. Dehsara and A. Abbassi, Mixed convection MHD flow of nanofluid over a non-linear stretching sheet with effects of viscous dissipation and variable magnetic field, MECHANIKA, Volume 18(4) (2012) 415-423.

17. F. Khani, A. Farmany, M. Ahmadzadeh Raji, Abdul Aziz and F. Samadi, Analytic solution for heat transfer of a third grade viscoelastic fluid in non-Darcy porous media with thermophysical effects,

18. Commun Nonlinear Sci Numer Simulat 14 (2009) 3867–3878.

19. A.J. Chamka , MHD flow of a uniformly stretched vertical permeable surface in the presence of heat generation/absorption and a chemical reaction, Int. Commun. Heat Mass Transfer 30 (2003) 413–422.

20. Afifi, MHD free convective flow and mass transfer over a stretching sheet with chemical reaction, Heat Mass Transfer 40 (2004) 495–500.

21. Postelnicu, Influence of chemical reaction on heat and mass transfer by natural convection from vertical surfaces in porous media considering Soret and Dufour effects, Heat Mass Transfer 43 (2007) 595–602.

22. R. Kandasamy and P.G. Palanimani, Effects of chemical reactions, heat, and mass transfer on nonlinear magnetohydrodynamic boundary layer flow over a wedge with a porous medium in the presence of ohmic heating and viscous dissipation, J. Porous Media 10 (2007) 489–502.

23. K. Sarit , Das SUSC, Yu. Wenhua, and T. Pradeep, Nanofluids Science and Technology. 1 edition, Honboken, NJ, John Wiley \& Sons, Inc, 2007.

24. J. Buongiorno, (March 2006), Convective Transport in Nanofluids, Journal of Heat Transfer (American Society Of Mechanical Engineers) 128 (3) (2010) 240.

25. W. Yu, D. M. France, J. L. Routbort, and S. U. S. Choi, Review and Comparison of Nanofluid Thermal Conductivity and Heat Transfer Enhancements, Heat Transfer Engineering, 29(5) (2008) 432-460 (1).

26. H.U. Kang, S.H. Kim and J.M. Oh, Estimation of thermal conductivity of nanofluid using experimental effective particle volume, Exp. Heat Transfer 19 (3) (2006)181–191.

27. V. Velagapudi, R.K. Konijeti and C.S.K. Aduru, Empirical correlation to predict thermophysical and heat transfer characteristics of nanofluids, Therm. Sci. 12 (2) (2008) 27–37.

28. V.Y. Rudyak, A.A. Belkin and E.A. Tomilina, On the thermal conductivity of nanofluids, Tech. Phys. Lett. 36 (7) (2010) 660–662.

29. H. Masuda, A. Ebata, K. Teramae and N. Hishinuma, Alteration of thermal conductivity and viscosity of liquid by dispersing ultra-fine particles, Netsu Bussei 7 (1993) 227–233.

30. J. Buongiorno and W. Hu, Nanofluid coolants for advanced nuclear power plants. Proceedings of ICAPP 05: May 2005 Seoul. Sydney: Curran Associates, Inc, (2005)15-19.

31. J. Buongiorno, Convective transport in nanofluids. ASME J Heat Transf, 128(2006)240-250.

32. W. A. Khan, and I. Pop, Free convection boundary layer flow past a horizontal flat plate embedded in a porous medium filled with a nanofluid, Journal of Heat Transfer, vol. 133(2011)9.

33. O.D. Makinde and A. Aziz, MHD mixed convection from a vertical plate embedded in a porous medium with a convective boundary condition, Intern. Journal of Thermal Sciences 49(2010)1813-1820.

34. H. B. Keller, A new difference scheme for parabolic problems. : Numerical solutions of partial differential equations, II (Hubbard, B. ed.).,New York: Academic Press, (1971)327–350.

35. H.F. Oztop and E. Abu-Nada, Numerical study of natural convection in partially heated rectangular enclosures filled with nanofluids, Int. J. Heat Fluid Flow 29 (2008) 1326–1336.

36. P.K. Kameswaran , S. Shaw , P. Sibanda and P.V.S.N. Murthy, Homogeneous.heterogeneous reactions in a nanofluid flow due to a porous stretching sheet, International Journal of Heat and Mass Transfer 57 (2013) 465–472.

37. R.K. Tiwari, M.N. Das, Heat tranfer augmentation in a two – sided lid – driven diffrentially heated square cavity utilizing nanofluids, Int. J. Heat Mass Transfer 50 (2007) 2002–2018.

38. S. Ahmad, A. M. Rohni, and I. Pop, Blasius and Sakiadis problems in nanofluids, Acta Mech. 218 (2011) 195–204.

39. T. Cebeci and P.Pradshaw, Physical and Computational Aspects of Convective Heat Transfer, New York:Springer, 1988.

40. M.A.A. Hamad, Analytical solution of natural convection flow of a nanofluid over a linearly stretching sheet in the presence of magnetic field, Int. Commun. Heat Mass Transfer 38 (2011) 487–492.

41. L.G. Grubka and K.M. Bobba, Heat transfer characteristics of a continuous stretching surface with variable temperature, ASME J. Heat Transfer 107 (1985) 248–250.